Original Article

EXPLORATION OF ANTI-MELANOMA POTENTIAL OF PHYTOCHEMICALS FROM *NYCTANTHES ARBORTRISTIS* THROUGH COMPUTATIONAL STUDIES

SHARMISTHA BANERJEE[1], MEENAKSHI BHARKATIYA[2] ⓘD, SURADA PRAKASH RAO[3], ISHITA BAGHEL[4], MADHURI BAGHEL[5]* ⓘD

[1]BME and BI, UTD, Chhattisgarh Swami Vivekanand Technical University, Newai, Bhilai, CG-491107, India. [2]Bhupal Nobles Institute of Pharmaceutical Sciences, Bhupal Nobles University, Udaipur-313001, India. [3]Columbia Institute of Pharmacy, Raipur, CG, India. [4]Foothill High School, 4375, Foothill Road, Pleasanton, CA-94588, India. [5]Apollo College of Pharmacy, Anjora, Durg, CG-491001, India
*Corresponding author: Madhuri Baghel; *Email: banchhormadhuri@gmail.com

ABSTRACT

Objective: The goal of the current research is to identify the dominant phytochemical from the plant *Nyctanthesarbor-tristis* Linn. and to investigate their binding affinities against the proteins BRaf Kinase mutant (3OG7) and Hsp90 Chaperone (2VCJ) that causes melanoma.

Methods: In this work, Schrodinger software was utilized to investigate the anti-cancer potential of phytochemicals *Nyctanthesarbor-tristis* against specific target proteins, namely BRaf Kinase mutant (3OG7) and Hsp90 Chaperone (2VCJ) Inhibitors.

Results: Based on the outcome of the docking investigation, phytochemicals that exhibited the highest binding affinity to the specified protein targets were subjected to induced fit docking and MM-GBSA computations using the Schrodinger Maestro version 2021.2 in prime module. According to the analysis, the compounds with the highest binding affinities for 2VCJ and 3OG7 are Arbortristoside D and Nicotiflorin, respectively. The compound that interacted with both proteins was Arbortristoside B. These phytochemicals appear to be more effective to the FDA-approved V600E-BRaf inhibitor Vemurafenib and Hsp90 Chaperone Inhibitor Diclonine.

Conclusion: One of the most common, deadly, and dangerous malignant diseases with a high global prevalence rate is melanoma (skin cancer). The present study may prove more helpful in developing an ideal targeted drug delivery system of phytochemicals obtained from plant *Nyctanthesarbor-tristis*for treatment of melanoma. This suggests that these substances could be evolved into highly effective anti-melanoma drugs.

Keywords: Skin cancer, *Nyctanthesarbor-tristis*, Dyclonine, Vemurafenib, Molecular docking, Induced fit docking

INTRODUCTION

Malignant melanoma is an aggressive form of skin cancer that accounts for approximately 75% of skin cancer-related deaths worldwide [1, 2]. According to American Cancer Society, estimate for melanoma in the United States for 2023 was about 97,610 new cases of invasive and 89,070 cases of in-situ melanoma will be diagnosed in United States, while 7,990 (approx) people are expected to die of melanoma Melanoma will be leading cause of death world wide.

Melanoma is reportedly affected by various environmental and genetic factors, such as ultraviolet exposure and carcinogenic BRAF mutations [3, 4]. Inspite of several available treatment modalities (surgery, radiation therapy, immunotherapy, and chemotherapy) [5, 6] to cure melanoma, phytochemicals have been recognized as better anti-cancer therapies to prevent or inhibit carcinogenesis because of its fewer side effects and better biocompatibility [7].

Synthetic chemicals are widely used as medicines in the treatment of diseases, encompassing various side effects. Different plants were explored as a source of bioactive agents for the treatment of ailments like cancer. Plants pose immense biological properties due to the presence of different chemical substances which perform several important physiological functions. Among 4,22,000 flowering plants reported from the whole world, more than 50,000 plants are reported to have medicinal and pharmacological uses. A rich diversity of medicinal plants is found in India [8].

Nyctanthesarbor-tristis (NTA) Linn. (Oleaceae), commonly known as 'parijat' is a common wild shrub flourishing in the sub-Himalayan tract in the states of Uttar Pradesh, Assam, Bengal, Madhya Pradesh and in the south upto Godavari [9]. *NTA* is a beautiful and fragrant plant. Its flowers bloom at night, drop off and fall early next morning for this reason, it is called as-sad tree‖. It is mainly characterized by the presence of phenylethanoid derivatives and iridoid derivatives. It is used in traditional medicine as stomachic, carminative, intestinal astringent, expectorant, in biliousness, piles, and various skin diseases and as hair tonic. It has also been reported to possess hepato-protective, anti-viral, antifungal and analgesic, anti-pyretic, ulcerogenic activities [10].

Juice of the leaf is used in chronic and bilious fever rheumatism as a laxative, diaphoretic and diuretic. The plant has been reported to be effective against leishmanial, viral and amoebic infections [11]. It is also been used in the Ayurvedic system of medicine for the cure of snake bite, bites of wild animals, cancer, sores, ulcers, dysentery, menorrhagia and obstinate sciatica. Leaves are responsible for some Central Nervous System (CNS) activities such as hypnotic, tranquilizing, local anesthetic antiasthmatic activities [12].

Vemurafenib has potent inhibitory effect and is selective for BRAF kinase [13]. It is used to treat diseases imposed on by V600E-BRAF. Despite these advances, a large number of patients experienced vemurafenib resistance, and reports have demonstrated keratoacanthoma and high rates of squamous cell carcinomas associated with identified inhibitors [14, 15]. HSP90 chaperones, including mutant B-raf, are essential for cell survival and advancement of malignancy. Thus, blocking HSP90 can effectively stop the signalling pathways that promote tumour growth and stop HSP90 from functioning in tumour cells [16].

Therefore, the current study focuses on targeting Hsp90 Chaperone protein 2VCJ and B-Raf Kinase mutant protein 3OG7. We investigated the anti-cancer properties of phytochemicals from *NTA* against these protein targets. Further, we performed structure-based screening of phytochemicals from *NTA* against skin cancer protein targets and combined molecular docking, quantum mechanical charge derivation (MMGBSA) in the binding site, followed by induced fit docking on the protein targets, which is responsible for producing melanoma cancer.

MATERIALS AND METHODS

Protein preparation and receptor grid generation

The three-dimensional (3D) structures of melanoma target proteins were retrieved from RCSB with Protein Data Bank (PDB) ids2VCJ (Hsp90

Chaperone Inhibitors, 2.50 Å resolution) [17] and 3OG7 at (B-Raf Kinase mutant, 2.45 Å resolution) [18-19]. The proteins were created using the Schrodingermodelling computations. The proteins' 3D structures have been imported using the "Protein preparation wizard" in accordance with the procedure described by Tutone *et al.* [20]. Missing hydrogen atoms, Heavy atoms, water molecules, metal ions, co-crystallized ligands and incomplete and/or terminal amide groups could all be present in a protein structure and the wizard treated the metals, corrected the bond ordering, rectified the formal corrections, removed the extra water beyond the 3 Angstrom limit of the het atom, and added the missing protons. The most stable state for the protein's ligand's potential ionisation states was determined using Epik [21]. The proteins were then optimised under regulated conditions employing the force field OPLS-2005 with a constrained RMSD tolerance of 0.3 [22].

The region wherein a receptor and ligand interacts is revealed through the establishment of receptor grids. The grid was built around the co-crystallized structure using the glide "receptor grid building" component of the Schrödinger suite [23]. The centroid that develops across the co-crystallized structure serves as a sign of the protein's active site [24, 25].

Ligands selection and preparation

The phytochemicals of *NTA* reported in literature [26, 27] were retrieved from Pubchem and are given in table 1. Eliminating salt and unnecessary hydrogen atoms is necessary to achieve a proper and legal protein-ligand docked complex. In order to prepare the ligands, the "LigPrep" module of the Schrodinger Maestro suite was applied to each ligand in the form of its 3D structure. Stereo-chemistries, desalting, and tautomer generation were chosen to obtain at least 32 conformations for each ligand and were optimized using Epikin pH between 7±2 and ring conformation [28].

Table 1: Reported phytoconstitutents of *NTA* with their pubchem id

S. No.	Phytoconstituent	Pubchem id
1.	4-hydroxy hexahydrobenzofuran-7-one	155803271
2.	6β-hydroxyloganin	158641
3.	Arachidic acid	10467
4.	Arborside C	182904
5.	Arborside D	101685135
6.	Arborsides A	182902
7.	Arborsides B	182903
8.	Arborsides C	182904
9.	Arbortristoside A	6442162
10.	Arbortristoside B	5459045
11.	Arbortristoside C	23955893
12.	Arbortristoside D	14632886
13.	Arbortristoside E	14632884
14.	Astragaline (Kaempferol 3-glucoside)	5282102
15.	Astraglin	5282102
16.	Benzoic acid	243
17.	Calceolarioside A	5273566
18.	Calceolarioside A	5273566
19.	crocetin	5281232
20.	Friedeline	91472
21.	Hentriacontane	12410
22.	Mannitol	6251
23.	Methyl salicylate	4133
24.	Nicotiflorin	5318767
25.	Nyctanthic acid	12313631
26.	Nyctanthoside	95224501
27.	Octacosane	12408
28.	Oleanolic acid	10494
29.	Oleic acid	445639
30.	Palmitic acid	985
31.	Phenyl acetaldehyde	998
32.	Rengyolone	10725564
33.	Vitamin C	54670067
34.	Υ-cymene	7463
35.	α-linolenic acid	5280934
36.	α-pinene	6654
37.	β-amyrin	73145
38.	β-digentiobioside-ester of α-crocetin (or crocin-I)	5281233
39.	β-monogentiobioside-ester of α-crocetin (or crocin-III	10461942
40.	β-monogentiobioside-β-D-monoglucoside-ester of α-crocetin (crocin-II),	9940690
41.	β-sitosterol	222284

Molecular docking (Rigid and flexible)

The Maestro12.8version tool was used in this investigation to perform rigid and flexible docking and to assess the binding affinities, ligand effectiveness, and inhibitory characteristic to the targets [29]. The ligands were docked to the active binding site of the melanoma proteins 2VCJ and 3OG7 using Extra precision-Glide XP mode, which binds to determine the flexibility of the ligand. The phytochemicals would be able to reliably bind to the protein and ligand hydrophobically, avoiding the consequences and getting high docking scores. The electrostatic interaction of the hydrogen bonds involved both the hydrophobic contact and the salt bridge contacts [30]. In order to predict precision of binding affinity of top-scoring *NTA* phytochemicals with anti-melanoma proteins, Induced fit docking (IFD) protocol was used. Using Glide and the Refinement module in Prime, IFD is an *in silico* method that accurately predicts ligand binding modes and related structural changes in the receptor [31].

Pose validation

In order to evaluate and validate the reproducibility of present computational method redocking of co-crystallized ligand into the

proteins' active regions was done. The RMSD (root mean square deviation) of the bound ligands were found to be 1.418Å, and 1.302Å

for 2VCJ and 3OG7, respectively and is illustrated in fig. 1. This demonstrates the reproducibility of the docking process.
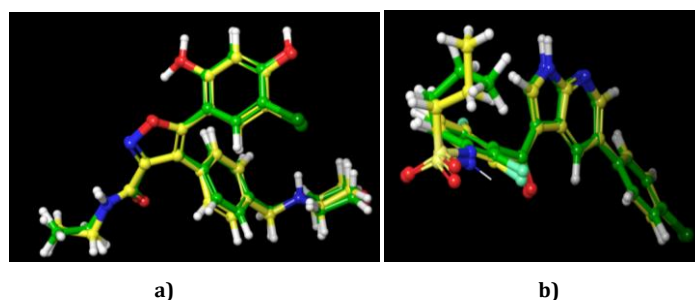

a) b)

Fig. 1: Superimposition of the re-docked conformation (Yellow) and crystal structure conformation (Green) a) 2VCJ b) b) 3OG7

Prime MM-GBSA (molecular-mechanics-generalized-born surface area) calculations

The ligand binding energy for each of the *NTA* phytochemicals and the recommended standard for inhibiting melanoma proteins was estimated using the MM-GBSA function in the Schrodinger Suite 2021 [32, 33]. This post-docking method is crucial because it exposes the proper ranking of ligands' binding and aids in accurately predicting the relative free binding energy [34]. Here, the PRIME module built into Maestro was used to calculate the free binding energies of the docked complexes by utilizing the XP docking methods [35].

RESULTS AND DISCUSSION

Discovery of novel therapeutics significantly depends on in situ approaches. They predict the experimental binding mechanism and affinity of ligand in the binding site of target [36, 37]. Glide XP-Molecular docking, MM-GBSA and IFD was successfully performed between the selected ligands (phytochemicals from *NTA*) and two melanoma protein targets (PDB ID: 2VCJ and 3OG7) using Schrodinger software. Molecular docking results of top 5 ligands with target proteins is summarized in table 2. Arbortristoside D and Nicotiflorininteracted efficiently with 2VCJ and 3OG7, respectively, with highest binding energy. All top 5 phytochemicals have higher binding score than the reference compounds Dyclonine [38] (-3.445) and Vemurafenib (-4.440). The scores were higher than the cocrystallizedligand also.

The XP and IFD scores of investigated phytochemicals with melanoma proteins revealed that for protein target 2VCJ; Arbortristoside D generated highest binding affinity with glide XP docking score of-8.793 kcalmol⁻¹ which is significantly higher than the reference compound Dyclonine (-3.445 kcalmol⁻¹) and cocrystallized ligand (-6.647). Arbortristoside D had the highest Glide emodel scores (-80.915 kcal mol⁻¹), followed by Arbortristoside B (-64.629 kcal mol⁻¹), which were higher than the reference Dyclonine(-44.289 kcalmol⁻¹)while the cocrystallized ligand had higher glide emodel score (-109.343 kcalmol⁻¹). The MMGBSA binding score was higest for cocrystallized ligand (-223.26), then for reference Diclonine (-198.08),

ArbortristosideD(-80.915 kcalmol⁻¹) and ArbortristosideB (-64.629 kcalmol⁻¹). The IFD scores were-437.52kcalmol⁻¹and-469.18 kcalmol⁻¹ for Arbortristoside D and Arbortristoside B, respectively. Both Arbortristoside D and Arbortristoside B formed 6 H-Bond (common interactions were with LYS58, ASP54 and THR184), while Dyclonine formed only 1 H-Bond (LYS 58) and cocrystallized ligand formed 4 H-Bonds (with THR148, LEU48, ASH93 and GLY97), 1 salt bridge (with ASP54), 1 Halogen bond with chloride residue (ASN51), and 1 Pi-Pi interaction (with LYS58). Khanpur *et al.* in 2014 reported the antiproliferative activity of the ethanol and ethyl acetate extracts of *N. abor-tristis* flowers against the MCF7 breast cancer cell line. The present result is in agreement with previous studies that the selected plant has already been reported to have anti-cancer activity [39].
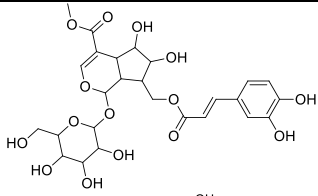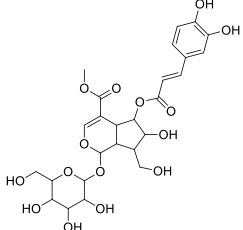
Forprotein target 3OG7, all the top five phytochemicals showed much higher binding score than the reference and cocrystallized ligand Vemurafenib with XP binding score of-4.440 kcal mol⁻¹. Among the phytochemicals, the decreasing order of XP binding scores were Nicotiflorin>Arbortristoside-B>Arbortristoside E>Arborside D>Astraglin. The glide emodel score was highest for Arbortristoside E (-87.130 kcal mol⁻¹), while the MMGBSA binding score was highest for reference Nicotiflorin (-99.63 kcalmol⁻¹). The IFD binding scores for Nicotiflorinand Arbortristoside-B were 548.99 kcal mol⁻¹ and-550.78 kcal mol⁻¹, respectively. Nicotiflorin showed 4 (LYS483, GLN530, CYS532, ASH594) while Arbortristoside-B and Vemurafenib (GLN530, CYS532, ASH594, TYR538, ASN580) showed 5 H-bond interactions with the same residues of protein target. The present study is in accordance with the finding that Arbortristoside A and B and iridoid glycosides are reported from seeds at 2.5 mg/kg in mice which possess anticancer activity against methylcholanthrene induced fibrosarcoma [40]. Additionally Vemurafenib also formed two salt bridges (with LYS483 and ASH594). Table 2 shows the top five scoring phytochemicals' Glide XP docking and MMGBSA scores as well as the kind of ligand-protein interactions and the implicated residue. Fig. 2 shows the 2D and 3D interactions of the top-scoring bioactives from *NTA* with protein targets. Table 3 shows the IFD score and structure of top two phytochemicals.
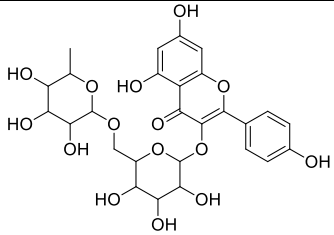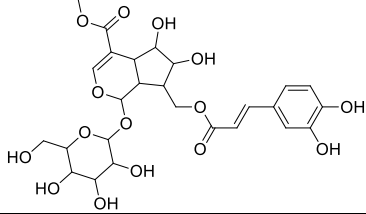
Table 2: Docking score, and MMGBSA score of top scoring (5) phytochemicals and reference with 2VCJ and 3OG7
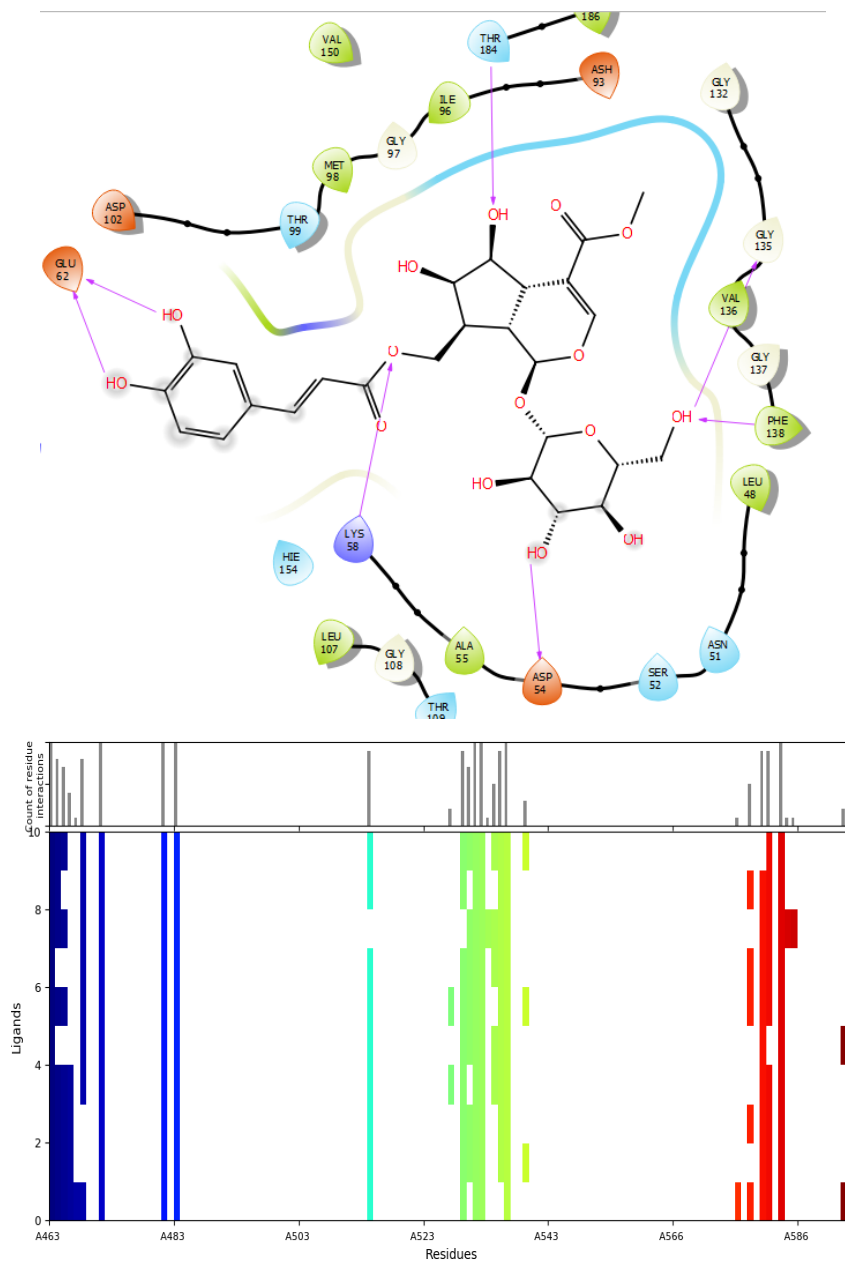
Protein pdb code	CID and compound name	Glide XP docking		MMGBSA d G bin D (kcalmol⁻¹)	Residues interactions	Types of bond formation
		Docking score	Glide emodel			
2VCJ	14632886 (Arbortristoside D)	-8.793	-80.915	-89.35	LYS58	H-bond with carboxyl
					ASP54	H-bond with hydroxyl
					GLU62	H-bond with hydroxyl
					PHE138	H-bond with hydroxyl
					GLY135	H-bond with hydroxyl
					THR184	H-bond with hydroxyl
	5459045 (Arbortristoside-B)	-7.798	-64.629	-35.33	LYS58	H-bond with oxygen
					ASP54	H-bond with hydroxyl
					GLY135	H-bond with hydroxyl
					THR184	H-bond with hydroxyl

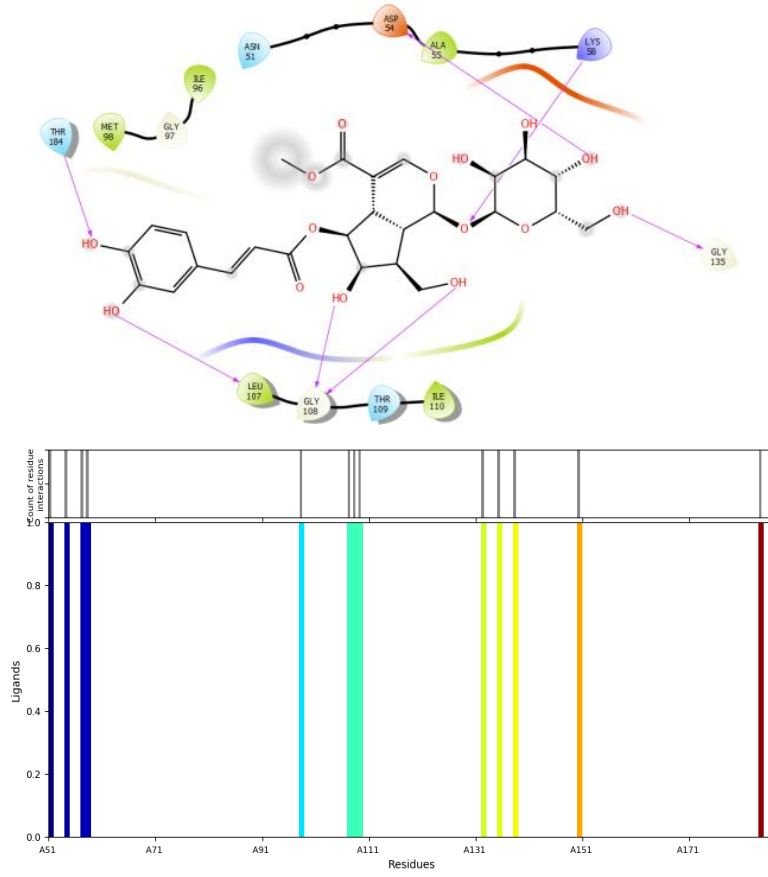| Protein pdb code	CID and compound name	Glide XP docking		MMGBSA d G bin D (kcalmol⁻¹)	Residues interactions	Types of bond formation
		Docking score	Glide emodel			
					LEU107	H-bond with hydroxyl
					GLY108	H-bond with hydroxyl
	101685135 (Arborside D)	-7.577	-75.665	-59.40	LYS58	H-bond with hydroxyl
					ASN51	H-bond with hydroxyl
					ASP102	H-bond with hydroxyl
	6442162(Arbortristoside A)	-7.361	-63.427	-66.41	ASP54	H-bond with hydroxyl
					ASN51SER50	H-bond with hydroxyl
						H-bond with hydroxyl
	23955893 (Arbortristoside C)	-6.653	-80.329	-76.01	LYS58	H-bond with hydroxyl
					GLY97	H-bond with hydroxyl
	3180 (Reference-Dyclonine)	-3.445	-44.289	-198.08	LYS58	H-bond with carbonyl
	Cocrystallized ligand (5-(5-chloro-2,4-dihydroxyphenyl)-N-ethyl-4-[4-(morpholin-4-ylmethyl)phenyl] isoxazole-3-carboxamide)	-6.647	-109.343	-223.26	ASP54	Salt bridge with ammonium
					ASN51	Halogen bond with chloride
					LYS58	Pi-Pi cataion
					LEU48	H-bond with hydroxyl
					ASH93	H-bond with hydroxyl
					THR184	H-bond with hydroxyl
					GLY97	H-bond with hydroxyl
3OG7	5318767 (Nicotiflorin)	-12.456	-75.433	-99.63	LYS483	H-bond with hydroxyl
					GLN530	H-bond with hydroxyl
					CYS532	H-bond with hydroxyl
					ASH594	H-bond with hydroxyl
	5459045 (Arbortristoside-B)	-12.455	-79.938	-77.29	GLN530	H-bond with hydroxyl
					CYS532	H-bond with hydroxyl
					ASH594	H-bond with hydroxyl
					TYR538	H-bond with hydroxyl
					ASN580	H-bond with hydroxyl
	14632884 (Arbortristoside E)	-11.288	-87.130	-93.20	CYS532	H-bond with hydroxyl
					CYS532	H-bond with carbonyl
					GLY534	H-bond with hydroxyl
					SER536	H-bond with hydroxyl
					SER465	H-bond with hydroxyl
	101685135 (Arborside D)	-11.246	-76.225	-81.41	CYS532	H-bond with hydroxyl
					CYS532	H-bond with carbonyl
					ASH594	H-bond with hydroxyl
					SER465	H-bond with hydroxyl
	5282102 (Astraglin)	-10.681	-73.205	-76.60	CYS532	H-bond with hydroxyl
					THR529	H-bond with carbonyl
					ASH594	H-bond with hydroxyl
					SER465	H-bond with hydroxyl
	Cocrystallized (N-(3-{[5-(4-chlorophenyl)-1H-pyrrolo[2,3-b]pyridin-3-yl]carbonyl}-2,4-difluorophenyl)propane-1-sulfonamide) or 4261125 (Reference-Vemurafenib)	-4.440	-58.869	-84.75	CYS532	H-bond with hydroxyl
					GLY596	H-bond with hydroxyl
					GLN530	H-bond with Nitrogen
					LYS483	H-bond with Sulfonyl oxygen
					LYS483	Salt bridge with amine
					ASH594	H-bond with Sulfonyl oxygen
					ASH594	Salt bridge with amine

Table 3: Structure and IFD score of top-ranked (2) compounds for target proteins 2VCJ and 3OG7

Protein	CID and compound name	IFD score	Structure
2VCJ	14632886 (Arbortristoside D)	-437.52	
	5459045 (Arbortristoside-B)	-469.18	

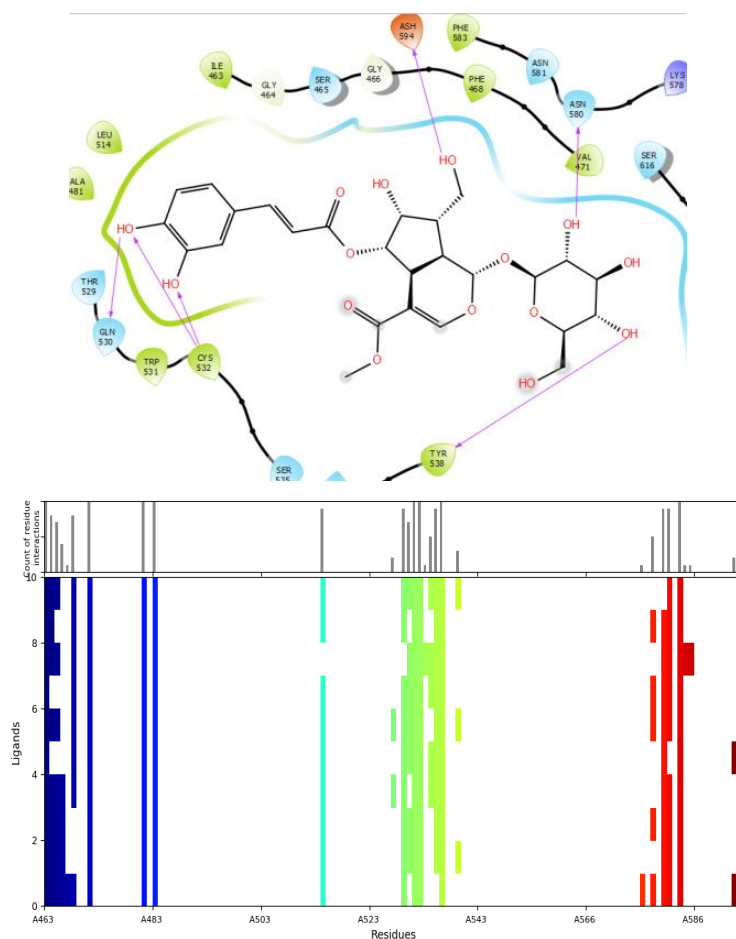| Protein	CID and compound name	IFD score	Structure
3OG7	5318767 (Nicotiflorin)	-548.99	
	5459045 (Arbortristoside-B)	-550.78	

a). 2VCJ (i) 14632889 (Arbortristoside D)

b). 2VCJ (ii) 5459045 (Arbortristoside-B)

c). 3OG7 (i) 5318767 (Nicotiflorin)

d). 3OG7 (ii) 5459045 (Arbortristoside-B)

Fig. 2: 2D interaction and fingerprint analysis of of top ranking bioactives (2) with protein targets a) 2VCJ and b) 3OG7

CONCLUSION

Patients suffering from advanced BRAFV600-mutant melanoma can benefit substantially from BRAF inhibitors; however, developing resistance is still prevalent. Preclinical research showed that concomitant use of the HSP90 inhibitor could eliminate resistance. Our study's findings made it abundantly evident that the target proteins 2VCJ can bind and interact strongly with Arbortristosides B and Arbortristosides D, as demonstrated by their binding energies than those of the other ligands we investigated. Similarly, Nicotiflorin and Arbortristoside B showed the best interaction with target proteins 3OG7. Based on the findings of our investigation, it is likely stated that Arbortristosides B is a potent antimelanomaphytodrug with the ability to interfere with both the investigated melanoma targets BRAF mutant (2VCJ) and HSP90 inhibitor (3OG7). Hence, it is believed that Arbortristosides B will be devoid of the resistance associated with the BRAF inhibitors. On the basis of the predictions of our *in silico* investigations, additional *in vitro* and *in vivo* experiments are required to determine the anticancer potential of these phytochemicals of *Nyctanthes Arbortristis* for their anti-melanoma activity.

FUNDING

Nil

AUTHORS CONTRIBUTIONS

Madhuri Baghel-Conceptulization, Data curation, Writing original draft and Supervision, Sharmistha Banergee-Data curation, writing original draft; Meenakshi Bharkatiya-Data curation, Writing an original draft, Supervision, Surada Prakash Rao-review and editing. Ishita Baghel-review and editing.

CONFLICT OF INTERESTS

Declared none

REFERENCES

1. Miller KD, Siegel RL, Lin CC, Mariotto AB, Kramer JL, Rowland JH. Cancer treatment and survivorship statistics, 2016. CA Cancer J Clin. 2016 Jun 2;66(4):271-89. doi: 10.3322/caac.21349, PMID 27253694.
2. Cummins DL, Cummins JM, Pantle H, Silverman MA, Leonard AL, Chanmugam A. Cutaneous malignant melanoma. Mayo Clin Proc. 2006 Apr;81(4):500-7. doi: 10.4065/81.4.500, PMID 16610570.
3. Markovic SN, Erickson LA, Rao RD, Weenig RH, Pockaj BA, Bardia A. Malignant melanoma in the 21st century, part 1: Epidemiology, risk factors, screening, prevention, and diagnosis. Mayo Clin Proc. 2007;82(3):364-80. doi: 10.4065/82.3.364, PMID 17352373.
4. Libra M, Malaponte G, Navolanic PM, Gangemi P, Bevelacqua V, Proietti L. Analysis of BRAF mutation in primary and metastatic melanoma. Cell Cycle. 2005 Sep 23;4(10):1382-4. doi: 10.4161/cc.4.10.2026, PMID 16096377.
5. Guevara Canales JO, Gutierrez Morales MM, Sacsaquispe Contreras SJ, Sanchez Lihon J, Morales Vadillo R. Malignant melanoma of the oral cavity. Review of the literature and experience in a peruvian population. Med Oral Patol Oral Cir Bucal. 2012 Mar 1;17(2):e206-11. doi: 10.4317/medoral.17477, PMID 22143709.
6. Vikey AK, Vikey D. Primary malignant melanoma, of head and neck: a comprehensive review of literature. Oral Oncol. 2012;48(5):399-403. doi: 10.1016/j.oraloncology.2011.12.014, PMID 22265336.

7. Jin S, Kim KC, Kim JS, Il Jang KI, Hyun TK. Anti-melanoma activities and phytochemical compositions of sorbus commixta fruit extracts. Plants (Basel). 2020 Aug 21;9(9):1-9. doi: 10.3390/plants9091076, PMID 32825598.

8. Parekh S, Soni A. Nyctanthes arbor-tristis: a comprehensive review on its pharmacological, antioxidant, and anticancer activities. J Appl Biol Biotechnol. 2020 Jan 10;8(1):95-104.

9. Jensen SR, Franzyk H, Wallander E. Chemotaxonomy of the oleaceae: iridoids as taxonomic markers. Phytochemistry. 2002 Jun 1;60(3):213-31. doi: 10.1016/s0031-9422(02)00102-4, PMID 12031440.

10. Rani C, Chawla S, Mangal M, Mangal AK, Kajla S, Dhawan AK. *Nyctanthes arbor-tristis* linn. (Night Jasmine): a sacred ornamental plant with immense medicinal potentials. Indian J Tradit Knowl. 2012 Jul 1;11(3):427-35.

11. Timsina B, Nadumane VK. Purification and evaluation of bioactive fractions for anticancer potentials from the flowers and leaves of *Nyctanthes arbor-tristis* L. Chiang Mai J Sci. 2016 Jul 2;43(1):100-11.

12. Khatune NA, Mosaddik MA, Haque ME. Antibacterial activity and cytotoxicity of *Nyctanthes arbor-tristis* flowers. Fitoterapia. 2001 Jun 1;72(4):412-4. doi: 10.1016/s0367-326x(00)00318-x, PMID 11395266.

13. Jang S, Atkins MB. Treatment of BRAF-mutant melanoma: the role of vemurafenib and other therapies. Clin Pharmacol Ther. 2014 Sep 30;95(1):24-31. doi: 10.1038/clpt.2013.197, PMID 24080641.

14. Zhan Y, Dahabieh MS, Rajakumar A, Dobocan MC, M'Boutchou MN, Goncalves C. The role of eIF4E in response and acquired resistance to vemurafenib in melanoma. J Invest Dermatol. 2015 Jan 23;135(5):1368-76. doi: 10.1038/jid.2015.11, PMID 25615552.

15. Martinez Garcia M, Banerji U, Albanell J, Bahleda R, Dolly S, Kraeber Bodere F. First-in-human, phase I dose-escalation study of the safety, pharmacokinetics, and pharmacodynamics of RO5126766, a first-in-class dual MEK/RAF inhibitor in patients with solid tumors. Clin Cancer Res. 2012 Sep 1;18(17):4806-19. doi: 10.1158/1078-0432.CCR-12-0742, PMID 22761467.

16. McCarthy MM, Pick E, Kluger Y, Gould Rothberg B, Lazova R, Camp RL. HSP90 as a marker of progression in melanoma. Ann Oncol. 2008 Mar;19(3):590-4. doi: 10.1093/annonc/mdm545, PMID 18037622.

17. Brough PA, Aherne W, Barril X, Borgognoni J, Boxall K, Cansfield JE. 4,5-Diarylisoxazole Hsp90 chaperone inhibitors: potential therapeutic agents for the treatment of cancer. J Med Chem. 2008 Jan 24;51(2):196-218. doi: 10.1021/jm701018h, PMID 18020435.

18. Bollag G, Hirth P, Tsai J, Zhang J, Ibrahim PN, Spevak W. Clinical efficacy of a RAF inhibitor needs broad target blockade in BRAF-mutant melanoma HHS public Access. 2010 Sep 30;467(3):596-9.

19. Choi WK, El-Gamal MI, Choi HS, Baek D, Oh CH. New diarylureas and diaryl amides containing 1,3,4-triarylpyrazole scaffold: Synthesis, antiproliferative evaluation against melanoma cell lines, ERK kinase inhibition, and molecular docking studies. Eur J Med Chem. 2011 Aug 12;46(12):5754-62. doi: 10.1016/j.ejmech.2011.08.013, PMID 22014559.

20. Tutone M, Virzi A, Almerico AM. Reverse screening on indicaxanthin from Opuntia ficus-indica as natural chemoactive and chemopreventive agent. J Theor Biol. 2018;455:147-60. doi: 10.1016/j.jtbi.2018.07.017, PMID 30030079.

21. Jang MK, Mashima T, Seimiya H. Tankyrase inhibitors target colorectal cancer stem cells via axin-dependent downregulation of c-kit tyrosine kinase. Mol Cancer Ther. 2020 Jun 6;19(3):765-76. doi: 10.1158/1535-7163.MCT-19-0668, PMID 31907221.

22. Shelley JC, Cholleti A, Frye LL, Greenwood JR, Timlin MR, Uchimaya M. Epik: a software program for pK(a) prediction and protonation state generation for drug-like molecules. J Comput Aided Mol Des. 2007;21(12):681-91. doi: 10.1007/s10822-007-9133-z, PMID 17899391.

23. Elokely KM, Doerksen RJ. Docking challenge: protein sampling and molecular docking performance. J Chem Inf Model. 2013;53(8):1934-45. doi: 10.1021/ci400040d, PMID 23530568.

24. Ajay Kumar TV, Athavan AAS, Loganathan C, Saravanan K, Kabilan S, Parthasarathy V. Design, 3D QSAR modeling and docking of TGF-β type I inhibitors to target cancer. Comput Biol Chem. 2018 Oct;76:232-44. doi: 10.1016/j.compbiolchem.2018.07.011, PMID 30077902.

25. Balachandran P, Kumar VAT, Parthasarathy V. Screening of potential anticancer compounds from sargassum wightii to target breast cancer-specific HER2 receptor using *in silico* analysis. Nat Prod J. 2016 Feb;6(2):108-15.

26. Sasmal D, Das S, Basu SP. Phytoconstituents and therapeutic potential of *Nyctanthes arbortristis* linn. Pharmacogn Rev. 2007 Jan;1(2):344-9.

27. Agrawal J, Pal A. Nyctanthes arbor-tristis linn–a critical ethnopharmacological review [Linn-a critical ethnopharmacological review]. J Ethnopharmacol. 2013 Apr 19;146(3):645-58. doi: 10.1016/j.jep.2013.01.024, PMID 23376280.

28. Sastry GM, Adzhigirey M, Day T, Annabhimoju R, Sherman W. Protein and ligand preparation: parameters, protocols, and influence on virtual screening enrichments. J Comput Aided Mol Des. 2013 Apr 12;27(3):221-34. doi: 10.1007/s10822-013-9644-8, PMID 23579614.

29. Meng XY, Zhang HX, Mezei M, Cui M. Molecular docking: a powerful approach for structure-based drug discovery. Curr Comput Aided Drug Des. 2011;7(2):146-57. doi: 10.2174/157340911795677602, PMID 21534921.

30. Schrodinger Release 2021-2. New York: Desmond, Schrodinger, LLC; 2021.

31. Sherman W, Day T, Jacobson MP, Friesner RA, Farid R. Novel procedure for modeling ligand/receptor induced fit effects. J Med Chem. 2006 Dec 23;49(2):534-53. doi: 10.1021/jm050540c, PMID 16420040.

32. Schrodinger Release 2021-2. New York: Prime, Schrodinger, LLC; 2021.

33. Wu Y, Hsieh TC, Wu JM, Wang X, Christopher JS, Pham AH. Elucidating the inhibitory effect of resveratrol and its structural analogs on selected nucleotide-related enzymes. Biomolecules. 2020 Aug 22;10(9):1-17. doi: 10.3390/biom10091223, PMID 32842666.

34. Lyne PD, Lamb ML, Saeh JC. Accurate prediction of the relative potencies of members of a series of kinase inhibitors using molecular docking and MM-GBSA scoring. J Med Chem. 2006 Jul 19;49(16):4805-8. doi: 10.1021/jm060522a, PMID 16884290.

35. Cumberworth A, Bui JM, Gsponer J. Free energies of solvation in the context of protein folding: implications for implicit and explicit solvent models. J Comput Chem. 2016 Mar 15;37(7):629-40. doi: 10.1002/jcc.24235, PMID 26558440.

36. Jayasurya BR, Swathy JS, Susha D, Sameer S. Molecular docking and investigation of *Boswellia Serrata* phytocompounds as cancer therapeutics to target growth factor receptors: an *in silico* approach. Int J Appl Pharm. 2023 Apr 21;15(4):173-83.

37. Sarvesh Galgale RZ, Pradeep Kumar A, Nithya M, Susha D, Sharma S. Molecular docking and dynamic simulation-based screening identifies inhibitors of targeted SARS-COV-2, 3-CLPRO and human ACE-2. Int J Appl Pharm. 2023 Aug 23;15(6):297-308.

38. Kandasamy S, Sahu SK, Kandasamy K. *In silico* studies on fungal metabolite against skin cancer protein (4,5-Diarylisoxazole HSP90 chaperone). ISRN Dermatol. 2012 Aug;2012:626214. doi: 10.5402/2012/626214, PMID 22991673.

39. Khanapur M, Avadhanula RK, Setty OH. *In vitro* antioxidant, antiproliferative, and phytochemical studyin different extracts of *Nyctanthesarbortristis* flowers. BioMed Res Int. 2014 May 2020;2:291271.

40. Susan T, Muzaffer A, Purushothaman KK. Inhibitory activity of arbortristoside a on fibrosarcoma in albino rats Arogya. 1986;12:122-30.